Supporting Information

Revisiting the role of hydrogen bonding in the strong dimer superexchange of a 2D copper(II) halide honeycomb-like lattice: Structural and magnetic study

Jeffrey C. Monroe,*[a] Christopher P. Landee[b], M. Àngels Carvajal,[c] Mercè Deumal,*[c] Melanie M. Rademeyer[d] and Mark M. Turnbull*[a]

[a]*Carlson School of Chemistry and Biochemistry, Clark University, 950 Main St., Worcester, MA 01610 USA*

[b]*Department of Physics, Clark University, 950 Main St., Worcester, MA 01610 USA*

[c]*Dept. Ciència de Materials i Química Física, & IQCTUB, Universitat de Barcelona, Martí i Franquès 1, Barcelona, E-08028*

[d]*Department of Chemistry, University of Pretoria, Private Bag X20, Hatfield 0028, South Africa.*

***Section 1. ^{1}H-NMR spectrum of* ligand H_2L^{2+}**

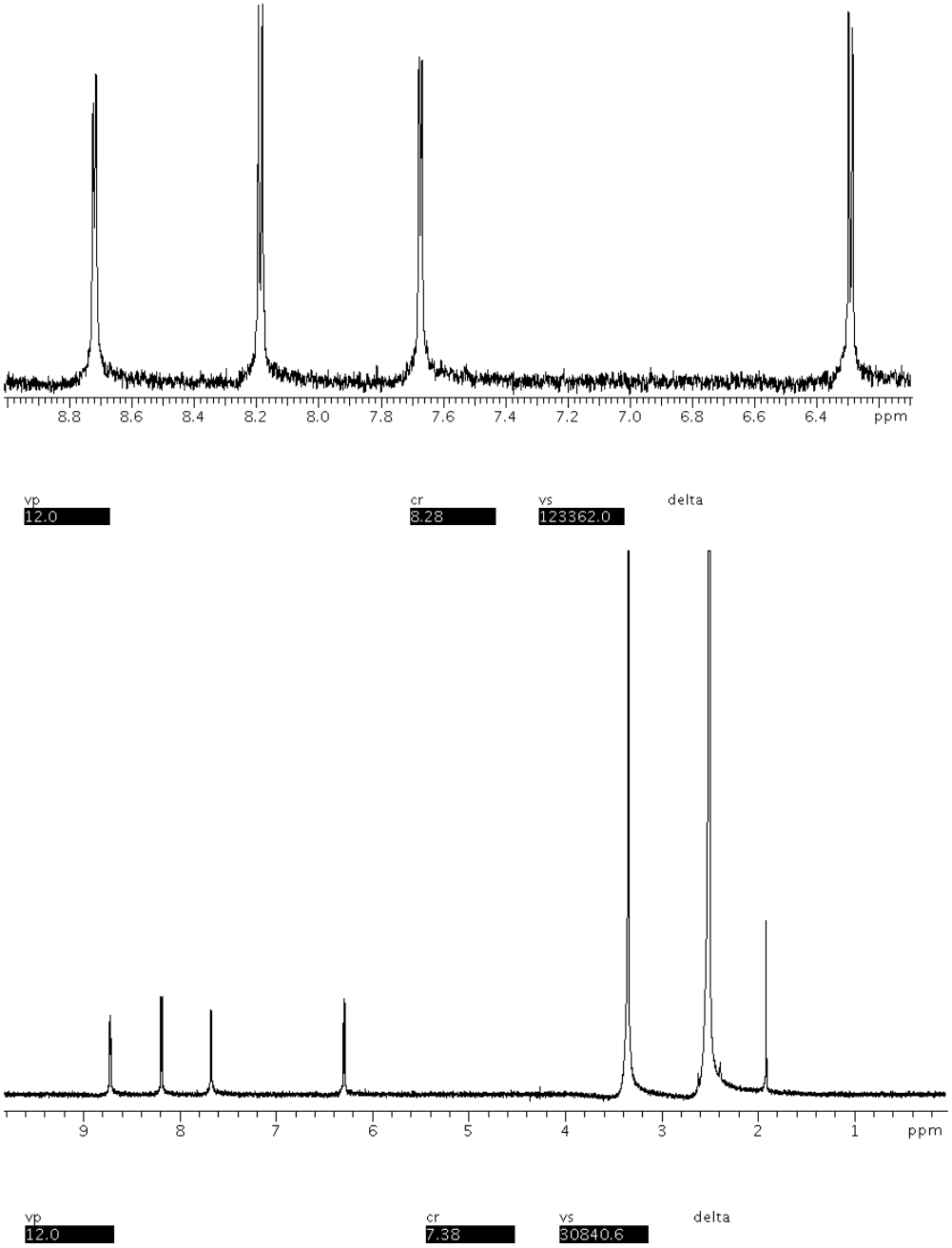

Figure S1. The ^{1}H-NMR spectrum of the ligand 1-(4'-pyridyl)pyridin-4-one dihydrate H_2L^{2+} (bottom) and an expansion of the aromatic region of the spectrum (top).

***Section 2. Powder X-ray diffraction of* 1**

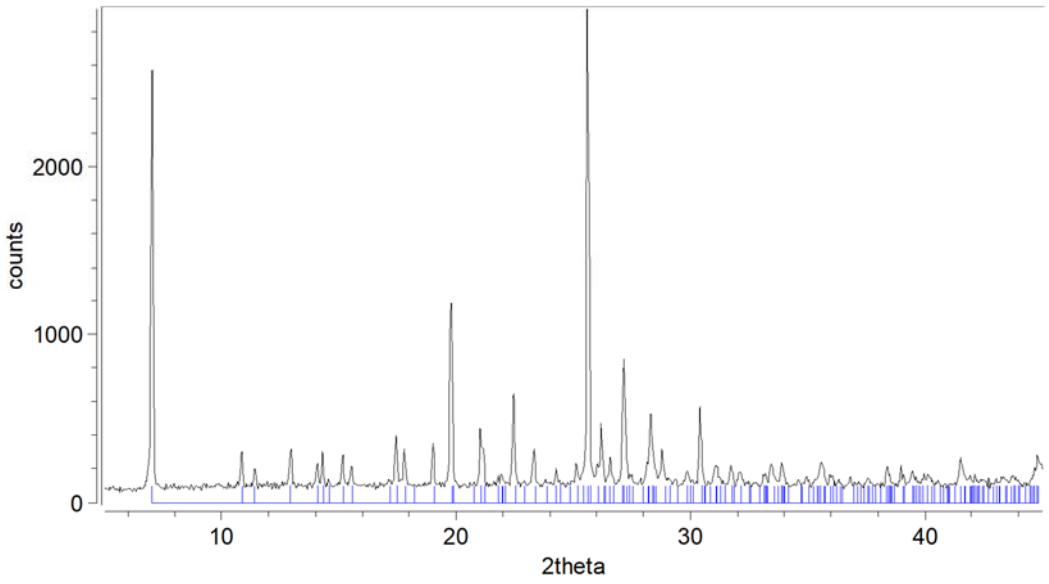

Figure S2. The powder X-ray diffraction pattern for the title compound. The positions of allowed reflections based on the single crystal structure are shown as blue tick marks.

Section 3. Best models used to fit the magnetic experimental data

The experimental magnetic susceptibility data were fit to the strong rung ladder model using an isotropic J Hamiltonian (see Eq. 1 and Figure S3a) where a negative value of J indicates antiferromagnetic interactions. In this regime the axial-equatorial chloride bridged chain is easily interpreted as the ladder rail ($J_{rail} \approx 1$ K, *vide infra*) while the hydrogen bonded dimer motif is interpreted as the ladder rung ($J_{rung} \approx 106$ K, *vide infra*).

$$\mathcal{H} = -J\sum[S_i^x S_j^x + S_i^y S_j^y + S_i^z S_i^z] \qquad (1)$$

The strong rung ladder model parameters are summarized in Table S3 (see Table 4 in main text). Addition of a Curie-Weiss correction parameter θ to account for interactions between motifs did not improve the quality of the fit. Attempts to employ the strong rail ladder model were unphysical, confirming the idea that the strong exchange occurs through the H-bonded dimers.

The Heisenberg dimer model with a Curie-Weiss correction for interdimer interactions (see Eq. 2), where X = % paramagnetic impurity, CC= Curie constant, θ is the Weiss constant and J is the exchange strength (K), also gave a satisfactory fit as shown in Figure S3b and Table S3.

$$\chi = 0.01X\left(\frac{CC}{T-\theta}\right) + (1-0.01X)\left(\frac{4CC}{3T}\right)\left(1+0.3333e^{J/T}\right)^{-1} \qquad (2)$$

This model suggests the axial-equatorial chloride bridged chains propagate weak exchange (θ ≈ -1 K), while the hydrogen bonded dimer interacts strongly (J ≅ 106 K). The fits to both models are acceptable however the spin-ladder model is a slightly better fit to χT(T) (R^2 χ(dimer) = 0.99968 , R^2 χT(dimer) = 0.99989 , R^2 χ(SP ladder) = 0.98866 , R^2 χT(SP ladder) = 0.99997).

Table S1. Fitting parameters for the dimer and strong rung ladder models with the standard error in parentheses. Fits to χT(T) are shown in brackets and do not include the Curie-Weiss correction θ.

Model	CC (emu-K/mol-Oe)	$J_{(rung)}$ (K)	$J_{(rail)}$ (K)	θ (K)	X (%)	R^2
Strong Rung Ladder	0.448(12) [0.4607(8)]	-105.8(7) [-106.96(16)]	2(7) [0.6(8)]	--- [---]	1.12(4) [1.42(3)]	0.98866 [0.99997]
Dimer	0.4498(7) [0.4441(5)]	-107.4(1) [-105.5(1)]	--- [---]	-1.22(3) [---]	1.61(1) [1.27(5)]	0.99968 [0.99989]

(a)

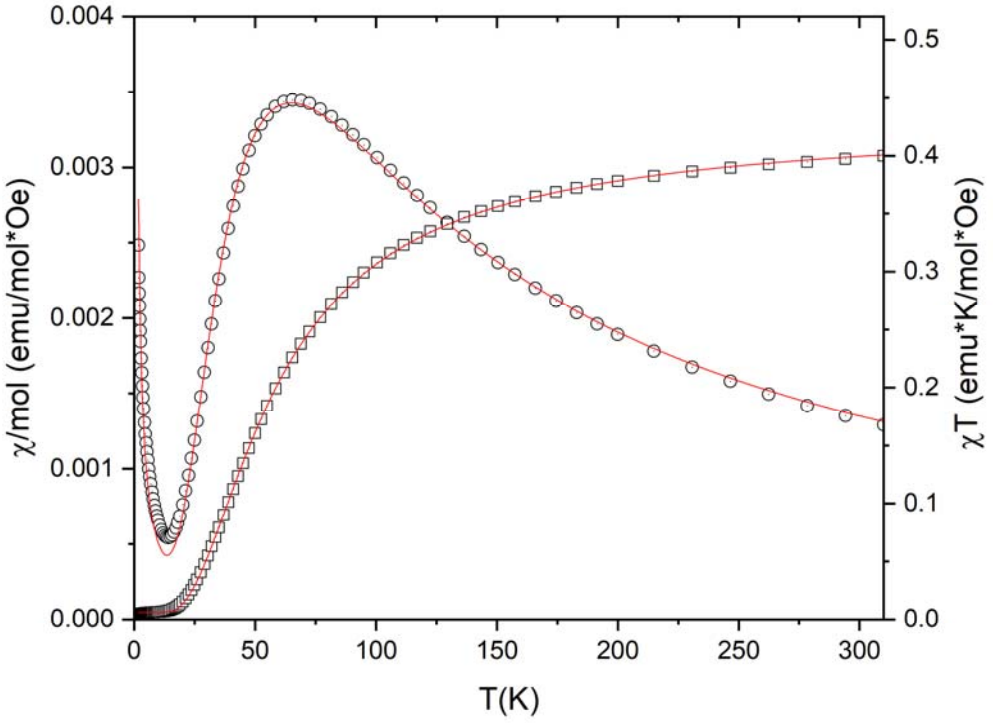

(b)

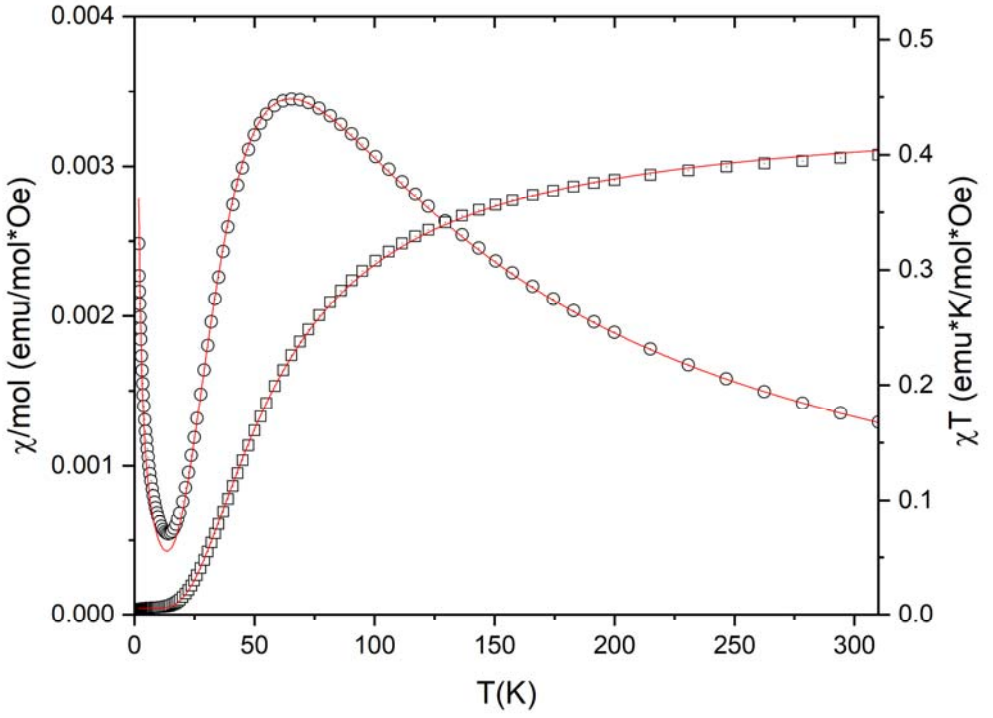

Figure S3. Left axis: χ vs. T (o) from 1.8 to 310K. Right axis: χT vs. T (□). Solid lines represent the best fit to the (a) strong-rung ladder model fit with a Curie-Weiss correction; (b) dimer model fit with a Curie-Weiss correction.

Section 4. Cluster models to evaluate J_{AB} magnetic interactions

Besides J_{44} (discussed in main text), all remaining magnetic interactions were evaluated using a bare dimer model (see Figures S4.a, S4.d, S4.f, S4.i and S4.k). The magnetic interaction between radicals at 6.181Å (J_{61}) is also calculated using a two $\mathbf{H_2L^{2+}}$ counterion dimer model (see Figure S4.b). A four-counterion dimer model is used to calculate J_{68} (see Figure S4.e), and J_{86} (see Figure S4.g). This model is extended up to a six-counterion dimer model to further evaluate J_{86} (see Figure S4.h). The addition of one chloride atom to a four-counterion (see Figure S4.c) and to a six-counterion (see Figure S4.l) dimer models enables to evaluate J_{61} and J_{899}, respectively. Finally, J_{895} is calculated using a model consisting of two radicals surrounded by two $\mathbf{H_2L^{2+}}$ counterions and two chloride anions (see Figure S4.j).

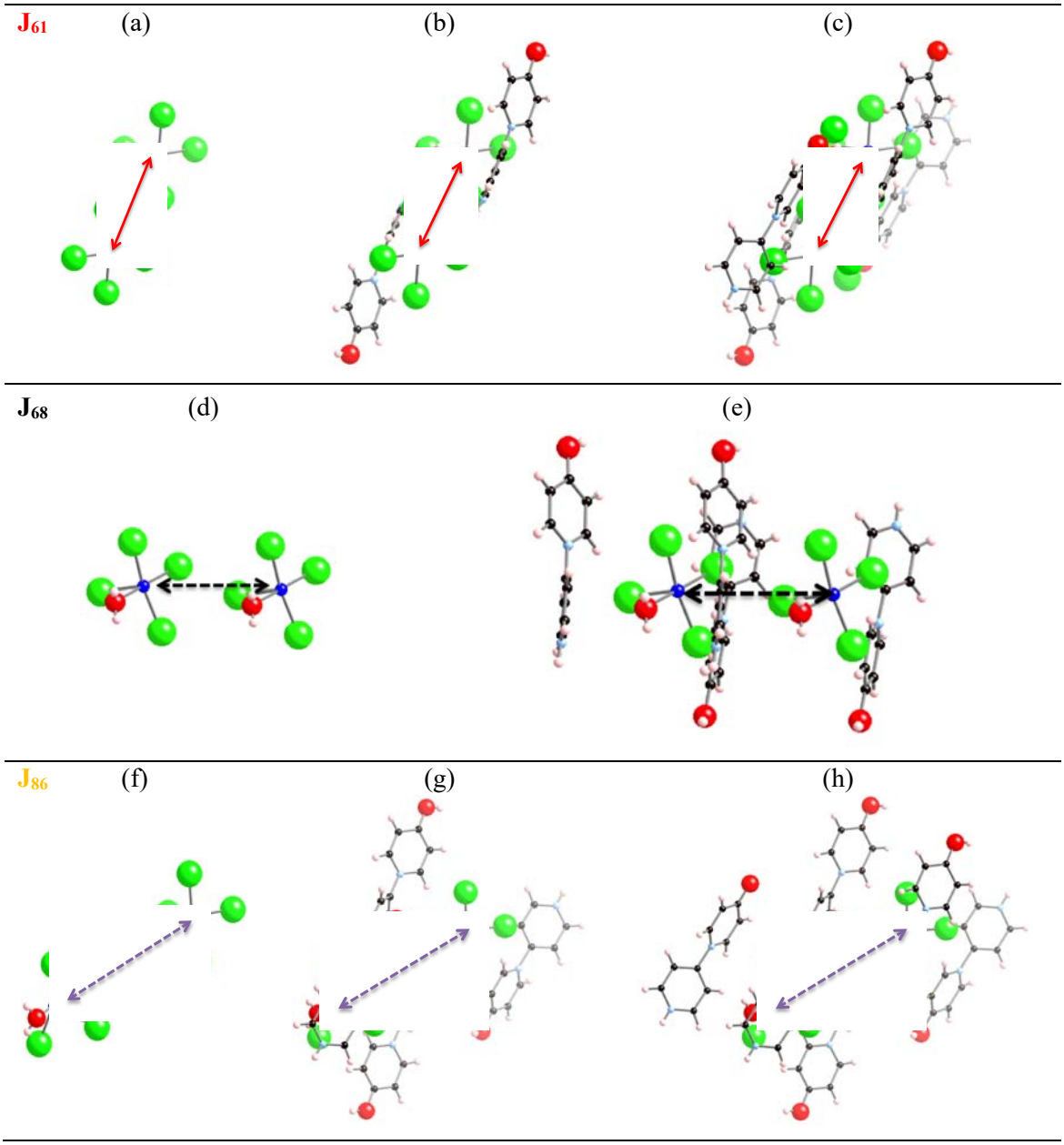

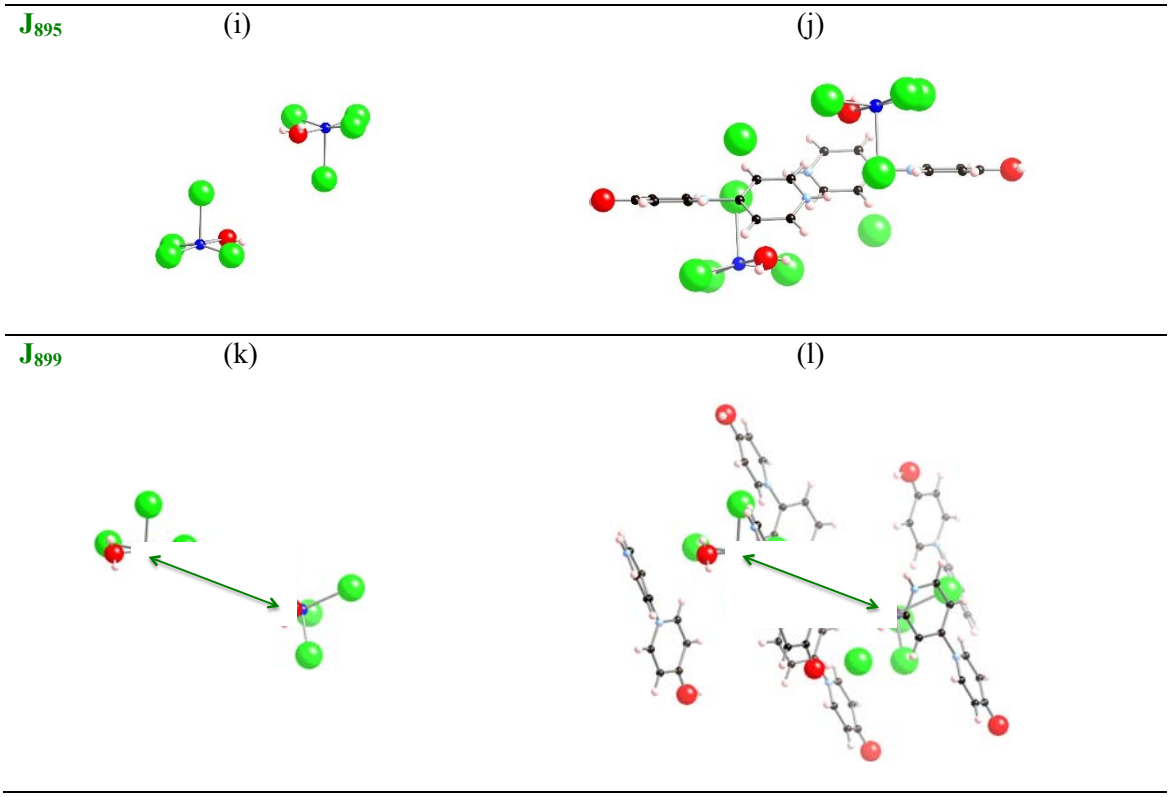

Figure S4. Models to evaluate J_{AB} exchange interactions between Cu-based radicals for all radical pairs within a Cu···Cu cutoff distance of 9.0Å.

Section 5. Magnetic models to calculate magnetic susceptibility χ(T)

The magnetic models used to calculate the magnetic susceptibility data include cyclic and open models. Both chain and 2D open models explored the cooperativity between magnetic couplings along *a*- and *b*-crystallographic axes. Chain models were enlarged from 6 to 10 to 14 radical centers along either *a* or *b*-axes (see Figure S5.1a). Two 2D open models were also contemplated: a 16-radical magnetic model whose honeycomb-motif is extended (i) 2 times along both *a*- and *b*-axes (see Figure S5.1b), and (ii) 3 times along the b-axis with the central motif then extended 2-times along a-axis (see Figure S5.1c). Besides open models, a 16-radical cyclic model was also considered (see Figure S5.1d).

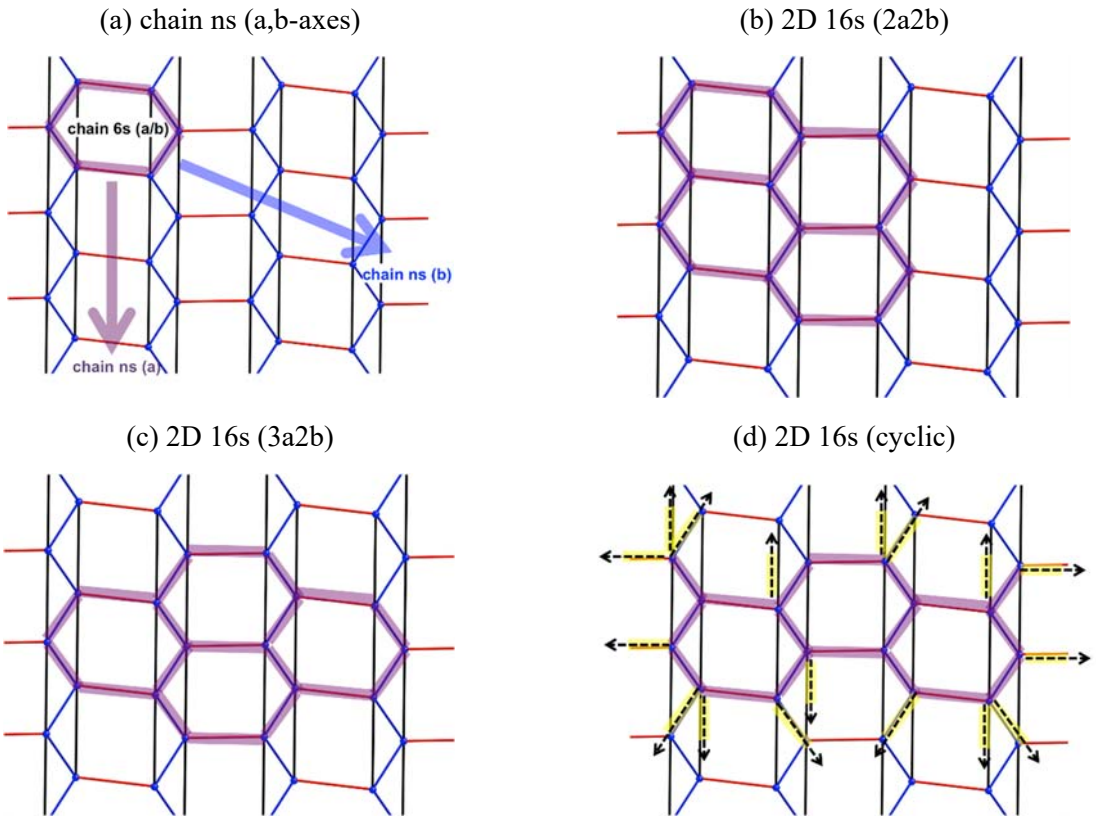

Figure S5.1. (a) Chain models. (b) 2D model resulting from extending the honeycomb-motif 2 times along both *a*- and *b*-axes. (c) 2D model resulting from extending the honeycomb-motif 3 times along the *b*-axis with the central motif then extended 2-times along *a*-axis. (d) 2D cyclic 16-radical model

Calculated χ(T) magnetic susceptibility data indicates that open chain models cannot reproduce the experimental data. As the open chain is enlarged from 6 to 10 to 14 radical centers along either *a* or *b*-axes (namely, chain *n*s (a) or chain *n*s (b), respectively, where *n* is the number of radicals considered in the model), the calculated χ(T) data get closer to the experimental values, but convergence to measures cannot be achieved, irrespective of using J_{AB} from dimer/trimer (Jd) or tetramer/trimer (Jt) calculations (see Figure S5.2a for Jd, and S5.2b for Jt).

Indeed the experimental magnetic susceptibility data for temperatures higher than 70K is qualitatively reproduced by 2D open magnetic models (see Figure S5.3). It is worth discussing that calculated χ(T) using J_{AB} interactions evaluated with tetramer/trimer (Jt) models reproduce better the experimental data (purple symbols for Jt and red symbols for Jd). However, the value of the magnetic susceptibility below 70K is overestimated by all the model but for the 2D cyclic model using Jt (see Figure S5.1d with J_{44}=17.0 cm^{-1}, J_{61}=-71.0 cm^{-1} & J_{68} =-14.6 cm^{-1} for model and empty purple circles in Figure S5.3 for calculated χ(T) data).

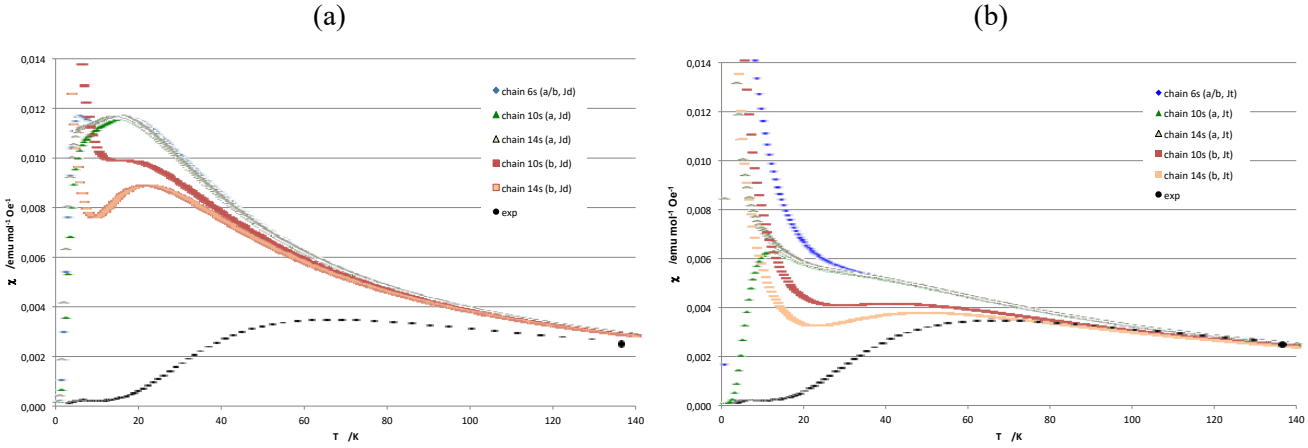

Figure S5.2. Calculated magnetic susceptibility using open chain models with J_{AB} obtained from (a) dimer/trimer (Jd) models, and (b) tetramer/trimer (Jt) models. Color code: blue diamond is honeycomb-6s magnetic motif (chain 6s); green triangle is chain 6s extended along *a*-axis (10 radicals, dark green; 14 radicals, light green); brown square is chain 6s extended along *b*-axis (10 radicals, dark brown; 14 radicals, light brown); black circles is experimental data.

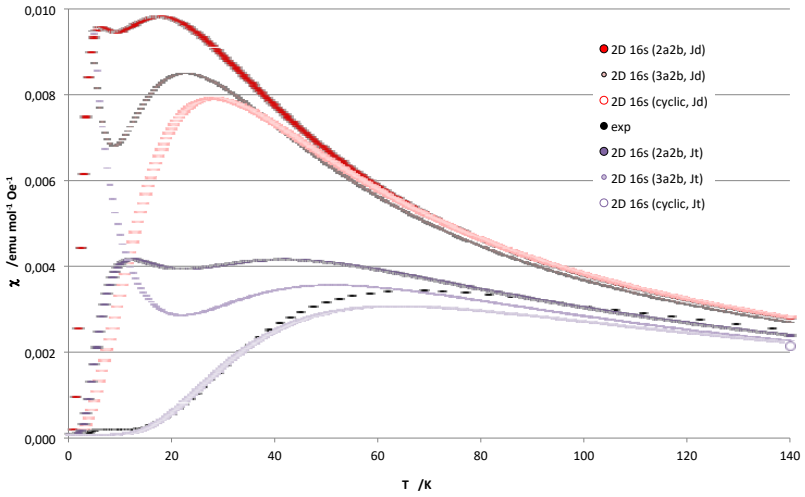

Figure S5.3. Calculated magnetic susceptibility using J_{AB} obtained from dimer/trimer (Jd, red symbols) models, and tetramer/trimer (Jt, purple symbols) models. Symbol code: 2D 2a2b (filled big circles), 2D 3a2b (filled small circles) and 2D cyclic (empty big circles); experimental data (black filled circles).

Finally, cyclic chain models are used. As expected, calculated data using magnetic models with J_{AB} obtained from dimer/trimer (Jd) models do not resemble the experimental χ(T) data at low temperatures (see Figure S5.4a). This behavior is in stark contrast with the χ(T) data calculated using cyclic chain models with J_{AB} from tetramer/trimer (Jt) models (see Figure S5.4b). There is obviously an improvement on the calculated χ(T) data as the chain length increases from 6 radicals to 14 radicals. Also the improvement is faster when enlarging along the *b*-axis because the overall magnetic response of **1** is AFM. It is thus clear that enlarging the magnetic model along the *a*-axis enhances the FM interactions by means of J_{44}, and accordingly it can disguise the actual magnetic response. In order to avoid this type of issues, the best minimal magnetic model we can choose must enlarge the 6-radical honeycomb magnetic motif evenly. Therefore, we will select the 16-radical 2D cyclic model using J_{AB} from tetramer/trimer (Jt) models to simulate the magnetic susceptibility of **1**.

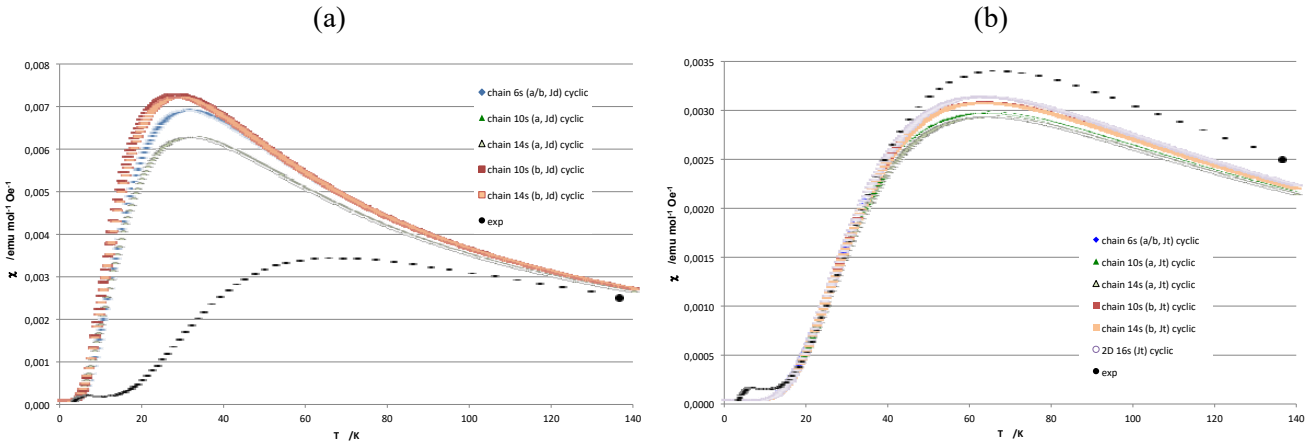

Figure S5.4. Calculated magnetic susceptibility using cyclic chain models with J_{AB} obtained from (a) dimer/trimer (Jd) models, and (b) tetramer/trimer (Jt) models. Color code: blue diamond is honeycomb-6s magnetic motif (chain 6s); green triangle is chain 6s extended along *a*-axis (10 radicals, dark green; 14 radicals, light green); brown square is chain 6s extended along *b*-axis (10 radicals, dark brown; 14 radicals, light brown); black circles is experimental data.